Soft Matter

PAPER

View Article Online
View Journal | View Issue

Cite this: *Soft Matter*, 2015, **11**, 4507

Preparation of Pickering emulsions stabilized by metal organic frameworks using oscillatory woven metal micro-screen

R. Sabouni† and H. G. Gomaa*

Received 18th April 2015,
Accepted 29th April 2015

DOI: 10.1039/c5sm00922g

www.rsc.org/softmatter

Uniform Pickering emulsions stabilized by metal organic frameworks (MOFs) MIL-101 and ZIF-8 nanoparticles (NPs) were successfully prepared using an oscillatory woven metal microscreen (WMMS) emulsification system in the presence and the absence of surfactants. The effects of operating and system parameters including the frequency and amplitude of oscillation, the type of nano-particle and/or surfactant on the droplet size and coefficient of variance of the prepared emulsions are investigated. The results showed that both the hydrodynamics of the system and the hydrophobic/hydrophilic nature of the NP influenced the interfacial properties of the oil–water interface during droplet formation and after detachment, which in turn affected the final droplet size and distribution. Comparison between the measured and predicted droplet size using a simple torque balance (TB) model is discussed.

Introduction

Emulsions stabilized by solid particles, also known as Pickering emulsions (PEs), have recently gained significant interest in many applications including pharmaceuticals, food products, cosmetics, and fuel processing.[1] They offer several advantages over conventional surfactant stabilized emulsions such as high stability attributed to an almost irreversible adsorption of the solid-particles onto the droplet interface which prevents their coalescence.[2,3] Another advantage is the potential for using benign solid-particles as stabilizers that could provide additional functionality and possibly avoid adverse effects that may be linked to using surfactants in cosmetics and pharmaceutical applications.[4] Furthermore, PE can also be used as a platform for the preparation of advanced material templates such as Janus colloids,[5] microspheres,[6] and composite microcapsules.[7]

Successful realization of the aforementioned benefits is strongly dependent on, first, the choice of the stabilizing particles and their characteristics and functional properties. Second, similar to surfactant stabilized emulsions, is also greatly influenced by the emulsification technique and its effect on the final emulsion particle size and distributions.

From the stabilizing particle selection point, there are several reports in the literature related to using a variety of materials for the preparation of PEs including metal oxides, cellulose, bacteria, latexes, and colloid silica, with the latter being the most commonly used.[8–11] From an emulsification technique point, most of the reported methods were based on conventional techniques such as high-pressure homogenization, ultrasonic devices, and rotor–stator systems. Such techniques however suffer from low energy efficiencies, broad droplet size distribution, and significant temperature and shear rise that could possibly have a negative impact on product functional properties. To overcome some of these limitations, membrane emulsification (ME) was proposed as an effective alternative.[12–14] Although there are a number of reports related to the use of ME for the preparation of conventional surfactant stabilized emulsions, limited information has been published on its application for the preparation of PEs.

The main objectives of this contribution are to first explore the potential of using new material namely metal organic frameworks (MOFs) as particle stabilizers for the preparation of PEs. MOFs are a new class of crystalline nanoporous compounds that have gained significant interest recently due to their attractive features in many applications including separation processes, catalytic reactions, and anticancer drug delivery, and can potentially offer many opportunities for the preparation of new materials based on PEs.[15–17] The second objective of this research is to investigate the feasibility and process characteristics of preparing such emulsions using a novel oscillatory membrane emulsification technique based on the dynamic membrane emulsification (DME) principles.[18–20] The design has the advantage of decoupling the continuous phase flow from the surface shear thus overcoming the relatively low dispersed phase concentration limitation typically encountered in conventional cross-flow

Department of Chemical and Biochemical Engineering, Western University, Ontario, Canada N6A5B9. E-mail: Hgomaa@uwo.ca

† Present address: Department of Chemical Engineering, American University of Sharjah, Sharjah, UAE.

membrane emulsification.[21–28] The characterization of the prepared emulsions as well as the MOF particles is presented. The effect of process parameters on particle size and distribution together with droplet formation mechanisms is discussed. The effect of combining both conventional surfactants and MOF nanoparticles on the emulsion properties is also investigated, and the results of the measured droplet sizes are compared to theoretical modeling predictions.

Experimental

Materials

Two particular types of MOF particles are investigated as emulsion stabilizers based on their reported excellent potential for applications in drug loading and delivery. First is ZIF-8, which is a tetrahedrally connected framework of composition $Zn(2\text{-MeIm})_2$ (2-MeIm = 2-methylimidazole), which belongs to zeolite imidazolate frameworks (Fig. 1a).

It displays high water stability and flexible sorption behaviour.[17] The pore structure is accessed through ~0.3 nm windows, and exhibits strong hydrophobic nature.[18] It combines the characteristics of both MOFs (tuneable pore size and high surface area) and Zeolite (high stability in aqueous solutions), which makes it an excellent candidate for drug delivery applications.[31–33] The second is Amine Materials of Institute of Lavoisier-101-Frameworks, NH_2-MIL-101 (Fe), or MIL-101, which is of the prototypical carboxylate-based MOFs that is composed of terephthalic acid linkers and Fe_3 salt, and has been recognized for its high drug loading and delivery capacities[34,35] (Fig. 1b). It has larger accessible pore windows (~0.6–1.0 nm), and is more hydrophilic than ZIF-8.

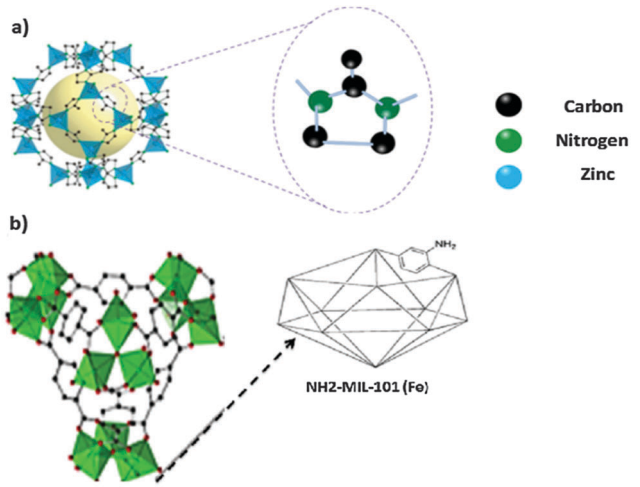

Fig. 1 Crystal structure of (a) ZIF-8 and (b) MIL-101.[29,30]

MIL-101 MOFs were prepared as shown before[36] by dissolving a mixture of NH_2–terephthalic acid (organic linker) and $FeCl_3$ (metal salt) in dimethylformamide (DMF) followed by microwave thermal treatment for a period of 30–90 seconds. The product was filtered and washed with DMF, then dried in a vacuum oven at 25 °C. ZIF-8 was purchased from Sigma-Aldrich and used without further purification.

The particles were characterized using X-ray diffraction analysis (XRD) and scanning electron microscopy (SEM). The XRD was carried out at ambient temperature using a Rigaku–MiniFlex powder diffractometer (Japan), and CuKα (λ for Kα = 1.54059 Å) over a 2θ range of 5° to 40° with a step width of 0.02°. The SEM images were taken using a Joel instrument (JSM 600F model, Japan) operating at an acceleration voltage of 10 keV (Fig. 2a and b). Non-ionic surfactant polyoxyethylene sorbitan monolaurate (Tween-20) obtained from Sigma-Aldrich was used for emulsions prepared using both surfactants and MOF NPs. The interfacial tensions were measured using a FTA1000 drop shape instrument, B system with FTA video drop shape software by First Ten Angstroms. The viscosities were measured using a rheometer model LVDE115. The physical properties of the systems used are listed in Table 1.

Experimental setup

The oscillatory woven metal micro-screen (WMMS) apparatus consists of a 1.5L Plexiglas rectangular container filled with the continuous phase, and an emulsification unit made up of two 35 mm × 25 mm WMMS sheets housed in the sides of the flat surface frame with a tapered end. The WMMS is made up of stainless steel plain weaves (38 μm pore size and 36% porosity) in which each weft wire passes alternately over and under each wrap wire and each wire passes alternately over and under each weft wire. The dispersed phase was injected through the micro-screen using a peristaltic pump (Pharmacia Fine Chemicals P-3 Peristaltic Pump) with a variable speed motor to control the flow rate. The oscillation frequency was controlled using a variable speed motor, while the amplitude was set using an eccentric system. This arrangement provided a wide range of frequencies

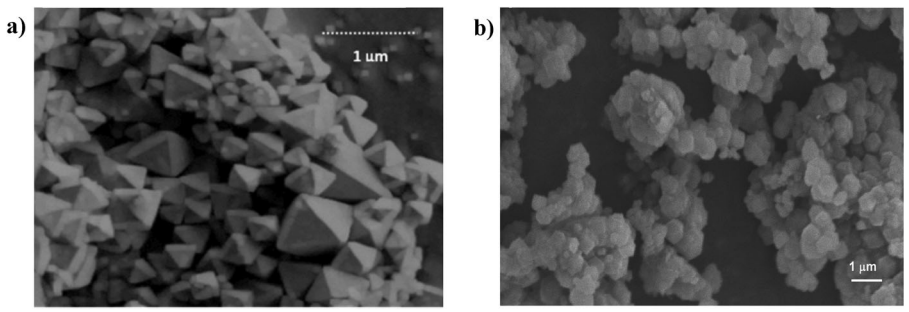

Fig. 2 SEM of (a) ZIF-8 and (b) MIL-101.

Table 1 Physical properties of the systems

Equilibrium interfacial tension (mN m^{-1})	
Oil–water	26.716
ZIF-8 in water–oil	0.381
ZIF-8 in oil–water	0.401
Oil–NH_2-MIL-101(Fe) in water	5.783
Oil–NH_2-MIL-101(Fe) in water & 1% Tween 20 in water	3.436
Viscosity (Pa s)	
Continuous phase (water)	0.0010
Continuous phase (ZIF-8 & water)	0.0015
Continuous phase (ZIF-8 1% Tween 20 & water)	0.0016
Continuous phase (NH_2-MIL-101(Fe) & water)	0.0013
Continuous phase (NH_2-MIL-101(Fe) 1% Tween 20 & water)	0.0014
Dispersed phase (oil)	0.55
Dispersed phase (ZIF-8 in oil)	0.50
Density (kg m^{-3})	
Continuous phase density (kg m^{-3})	1000
Dispersed phase density (kg m^{-3})	920
NH_2-MIL-101(Fe) NP physical properties	
Chemical formula	$C_6H_7FeNO_4$
Particle size (μm)	0.2
Density (kg m^{-3})[37]	620
HBL	both
ZIF-8 physical properties	
Chemical formula	$C_8H_{10}N_4Zn$
Particle size (μm)	0.5
Density (kg m^{-3})[38]	1450
HBL[17]	Hydrophobic

and amplitudes (f = 0–20 Hz, and a = 0–20 mm). Fig. 3 shows a schematic representation of the experimental apparatus.

Emulsion preparation and characterization

All emulsions were prepared by dispersing 12.5 mL of commercial vegetable oil in 400 mL of distilled water and 100 mg of nanoparticles. The latter were stirred in distilled water for 15 minutes before each experiment to ensure homogenous distribution. For combined surfactant-nanoparticle (NP) stabilized emulsions, 1% of Tween 20 was added to the continuous aqueous phase together with the NP. At the end of each experiment, 100 mL of sample was collected for emulsion droplet characterization. The apparatus was cleaned and rinsed thoroughly with distilled water after each experiment to eliminate any cross-contamination.

The observation and characterization of emulsions were done using a digital microscope (Ziess M2 1256 Microscope) and a video camera. The size distributions were estimated by image analysis. The average droplet size d was measured from 50–100 droplets immediately after each experiment. The droplet size distribution of each sample was measured using the coefficient of variation (CV) for n droplets given as,

$$\mathrm{CV} = \frac{1}{d}\sum_{i}^{n}\left[\frac{(d_i - d)^2}{n}\right]^{1/2} \quad (1)$$

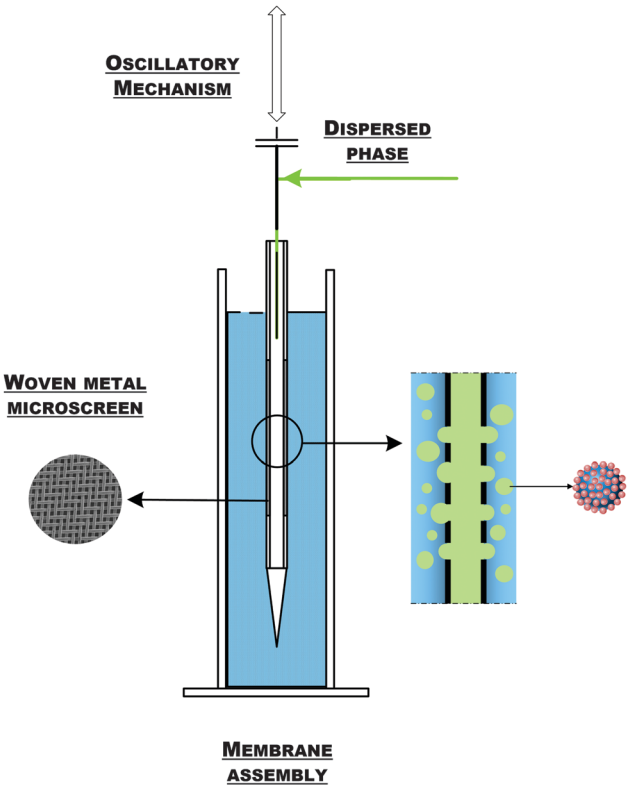

Fig. 3 The oscillatory woven metal-screen (WMMS) apparatus.

Results and discussion

Fig. 4 shows typical microscopy images and droplet size distribution of the formed emulsions. In almost all cases, the droplet size distribution was essentially monomodal and Gaussian in appearance.

The produced emulsions had a long shelf life with no evidence for droplet coalescence or ripening for over six months as shown in Fig. 5. This clearly demonstrates the effectiveness of using MOFs as particle stabilizers for the preparation of PEs.

Effect of nanoparticles (NPs)

The presence of NPs with affinity to the dispersed phase affects an emulsification process by their adsorption at the interface and the modification of the interfacial free energy due to the replacement of fluid–fluid with particle–fluid surface area. The reduction of the shared area between the phases creates a physical barrier to droplet coalescence, thus enhancing the emulsion stability. If the free energy reduction due to particle adsorption is large compared to thermal and external forces due to for example shear stresses in the flow field, particle adsorption can become almost irreversible. In the absence of NPs, the thermodynamic state is,

$$\Delta E = A\gamma_o - NE_d \quad (2)$$

in which ΔE is the change in the total interfacial free energy, γ_o is the interfacial tension of the bare interface, N_p is the number of NPs in a given interfacial area A, and E_d is the desorption energy required to remove one NP from the interface given by,

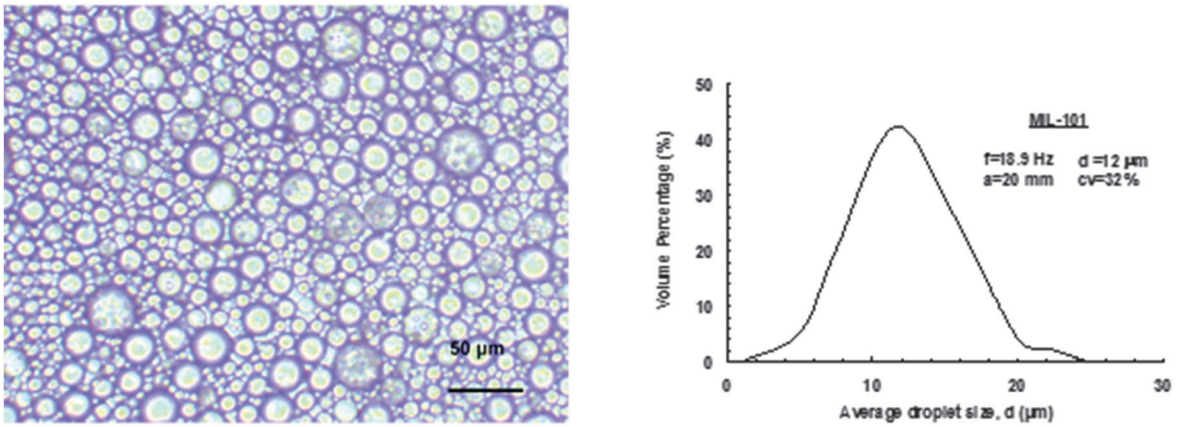

Fig. 4 Microscopy image and droplet size distribution of emulsions prepared using MIL-101NPs.

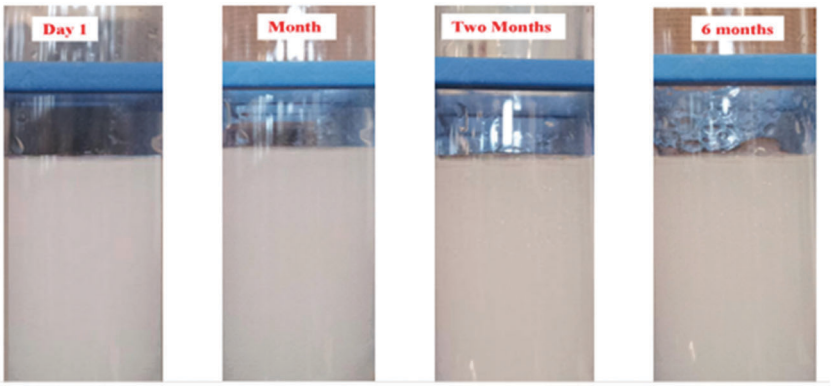

Fig. 5 Stability of the formed emulsions over six months using ZIF-8 NPs (f = 18.9 Hz, a = 6 mm).

$$E_d = \pi R^2 \gamma_o (1 - |\cos\theta|)^2 \quad (3)$$

where R is the particle radius and θ is the particle contact angle. It can be seen that increasing the size of the NP leads to larger surface coverage and higher desorption energy, and therefore larger interfacial energy reductions. Previous investigations have also shown that NP–NP interactions can affect its configuration at the liquid–liquid interface, which in turn affects the surface pressure and interfacial energy.[39] In this work, ZIF-8 and MIL-101 NPs were used as emulsion stabilizers. The former has larger average particle size and higher hydrophobic nature than the latter. Such differences would be expected to result in a stronger affinity of ZIF-8 NPs to the oil–water interface than MIL-101 NPs, and may possibly explain its stronger effect on droplet size and stability as will be discussed latter.

Effect of oscillations on droplet size

In a drop-by-drop emulsification, droplet detachment occurs mainly when the shear caused by the drag force F_d created by the relative motion between the fluid and the surface exceeds the interfacial tension holding force F_s that keeps the droplet attached to the pore. For particle stabilised emulsions, and assuming that particle adsorption is thermodynamically favoured, the kinetics for particle barrier formation must be matched with the drop-by-drop formation process to provide sufficient stability at the membrane surface to prevent coalescence. If the particle is weakly attached, which strongly depends on the particle affinity to the surface, it could diffuse away depending on the system characteristics and hydrodynamics.

Fig. 6a and b show the effect of oscillation frequency and amplitude on droplet size and distribution for emulsions prepared using ZIF-8. As can be seen, increasing the oscillation intensity decreases the emulsion droplet size as well as its polydispersity. This is due to the fact that higher oscillation results in increasing relative velocity between the fluid and the surface leading to an increase of drag force acting on the formation of droplets. This in turn will lead to detachment of smaller droplets, and reduce the probability of its coalescence at the pores, as well as breakage after detachment.

The effect of the dispersed phase flux on the droplet size is shown in Fig. 6c, which as can be seen, results in the increasing average droplet size. Such an effect could be attributed to the droplet detachment process, which is not infinitely fast, but requires a certain time. During that time, the droplet volume increases with the increasing dispersed phase injection rate to values larger than the critical detachment size determined by force balance.

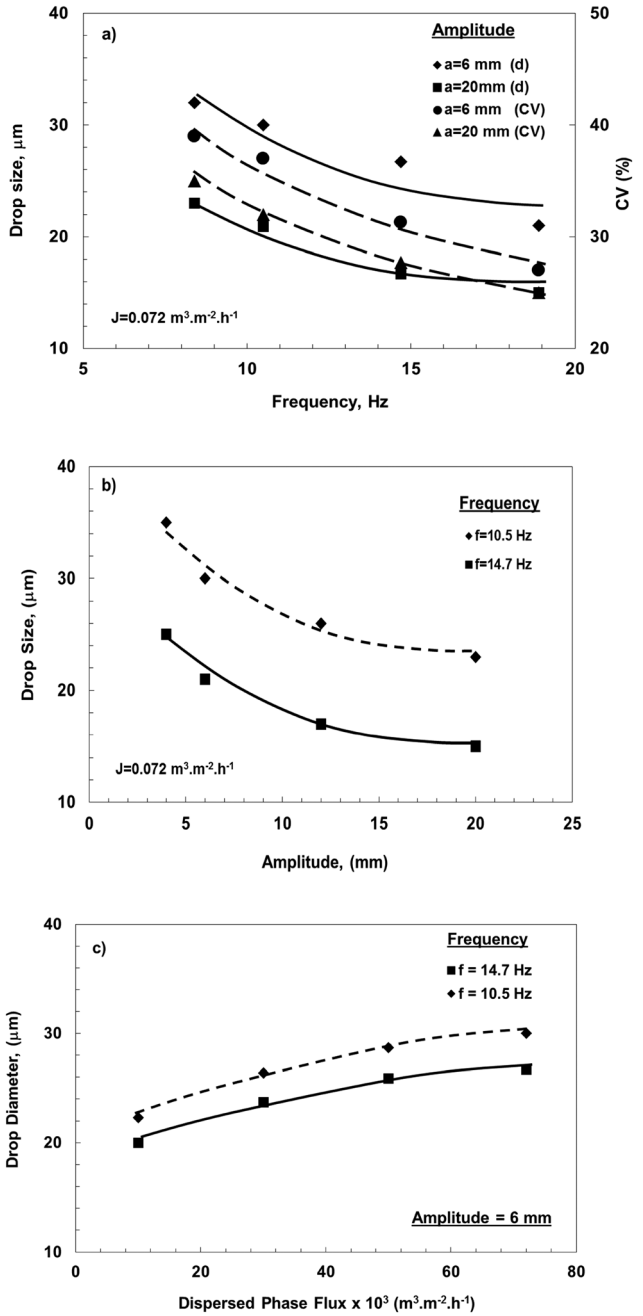

Fig. 6 Variation of droplet size and distributions for emulsions stabilized using ZIF-8. Effect of: (a) frequency, (b) amplitude, and (c) dispersed phase flux.

To further investigate whether the oscillation effect on particle diffusion towards the formation of droplets may have contributed to the improved CV values, we conducted a set of experiments with ZIF-8 NPs dispersed in the oil phase as an emulsion stabilizer. Under such conditions, the NPs are readily available at the oil–water interface during droplet formation, thus eliminating the probability of diffusional limitation from the bulk to the interface during droplet formation if any.

Fig. 7a and b show the change in droplet size and distribution with oscillation for these experiments together with results for emulsions prepared using ZIF-8 NPs dispersed in the continuous aqueous phase. It can be seen that there is hardly any difference between the two, which indicates that the convective flow field from the oscillatory motion provided sufficient particle flux to the growing droplet and that particle stabilization is not diffusion limited.

The effect of oscillations on the droplet size and distribution for emulsions produced using MIL-101 NPs is shown in Fig. 8a and b, respectively. As can be seen, the general trend for the effect of frequency on droplet size and distribution is similar to that observed for emulsions stabilized with ZIF-8 NPs. The effect of amplitude on the emulsion uniformity however was opposite, where higher CV values were observed as the amplitude increased. Furthermore, a comparison between MIL-101 and ZIF-8 results showed the latter to be more uniform (lower CV values), particularly at higher oscillation intensities. Such observations may suggest that the mechanisms affecting the final droplet size and distribution in one case may be different from those at work in the other.

A possible explanation for such phenomena may be attributed to the fact that NPs stabilize an emulsion if they remain strongly attached to the droplet surface, which varies depending on their binding force compared to other mobilization forces. The latter include thermal energy, which in most cases is much smaller than adsorption energy, leading to the commonly accepted argument of irreversible adsorption. Thermal energy, however, may not be the only factor affecting NP attachment, since other forces related to the hydrodynamics of the system, such as shear stresses and flow eddies, could also play a nontrivial role in particle mobilization. This phenomena can occur any time leading to particle removal from the droplet surface and possible coalescence of the latter to larger sizes, which in turn can be fragmented due to shear stresses, or chaotic eddy structure during shear reversal in oscillatory flows. This may explain the observed results since the higher hydrophobic nature of ZIF-8 and its stronger affinity to the oil–water interface could have resulted in the formation of smaller and more stable droplets that resisted further breakage at higher oscillatory shear. MIL-101 on the other hand, and due to its less hydrophobic nature and possible lower droplet interface affinity, would be easier to detach from a droplet surface under the influence of the surrounding hydrodynamic forces leading to the formation of larger droplets. Such droplets will have higher tendency for breakage to smaller satellite ones, particularly at higher oscillation intensities leading to the broadening of the formed emulsion size distribution. Similar results have been reported previously when using high shear rates.[28]

Effect of combining surfactants and nanoparticles

Although there are valuable information in the literature on the interfacial properties of oil–water systems in the presence of surfactants and NPs, particularly hydrophilic silica, the results suggest that the effect on the final emulsion properties depends strongly on the systems, the NP–surfactant interactions both at the droplet surface and in the bulk,[40,41] as well as the preparation technique.[42–45] For example, surfactant adsorption on the NPs may result in particle agglomeration

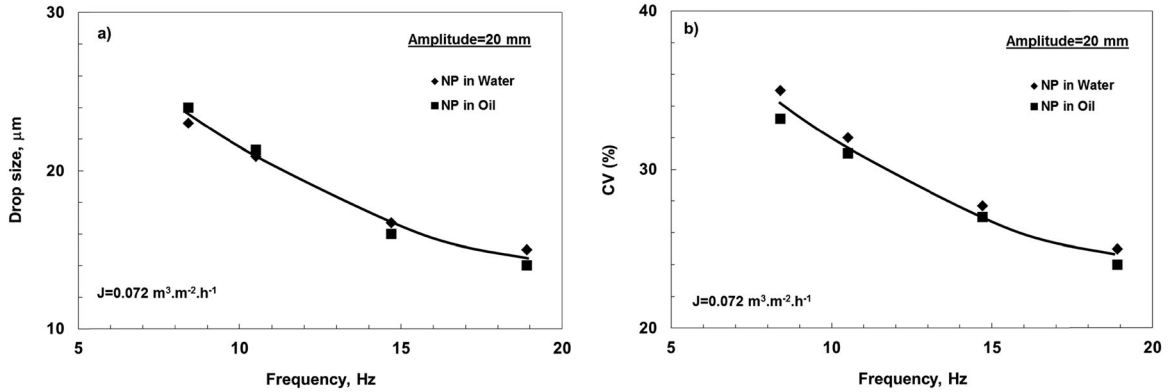

Fig. 7 Comparison between emulsions prepared using ZIF-8 in oil and water. Effect of oscillation frequency on (a) droplet size and (b) size distribution (CV).

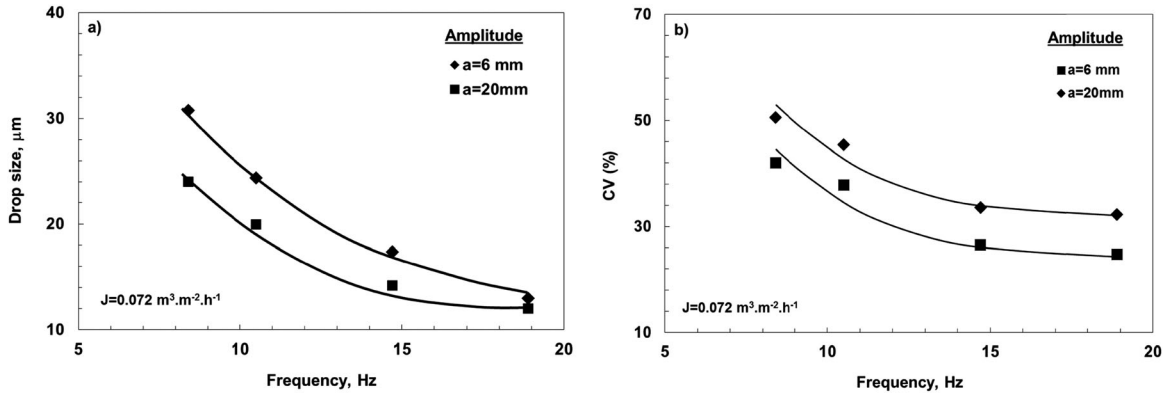

Fig. 8 Characteristics of emulsions stabilized using MIL-101. Effect of oscillation frequency on: (a) droplet size and (b) size distribution (CV).

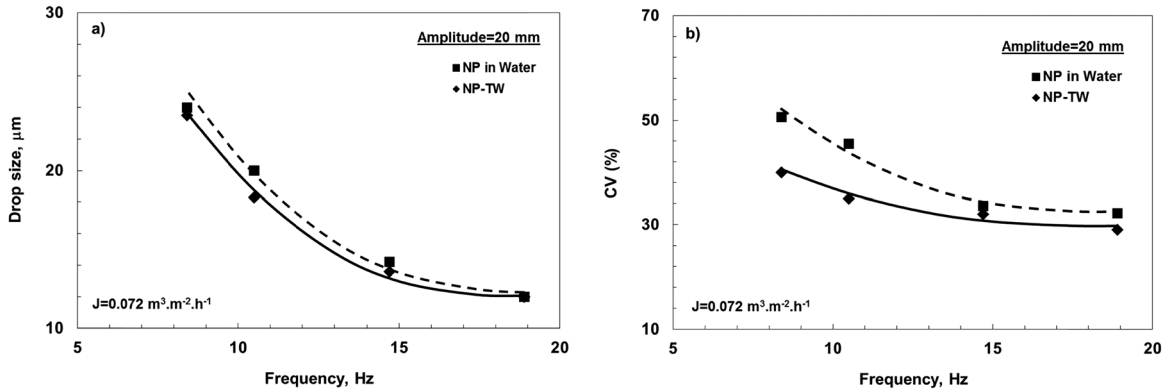

Fig. 9 Emulsions stabilized with MIL-101 in the presence of the Tween-20 surfactant. Effect of oscillation frequency on (a) droplet size and (b) size distribution (CV).

and adsorption of agglomerates at the oil/water interface leading to improved emulsion stability. On the other hand, surfactants which are bound onto the NP surface may not be effective in lowering the interfacial tension compared to free ones. The energy gained by binding the surfactants onto a NP is countered by the entropic penalty of confining the surfactants onto the NP surface as well as the energy penalty of removing the surfactant from the oil–water interface to the NP. Increasing surfactant concentration could also result in displacing the NPs from the oil/water interface which may affect the emulsion droplet size and distribution.[46] Furthermore, when particles decorated with various molecules are considered, particle–particle interactions could also have an effect on the interfacial energy.[39] Fig. 9a and b show representative results of the oscillation effect on droplet size and distribution of emulsions stabilised by the Tween-20 surfactant and MIL-101 NPs as compared to emulsions prepared using NPs alone, under the same oscillatory conditions.

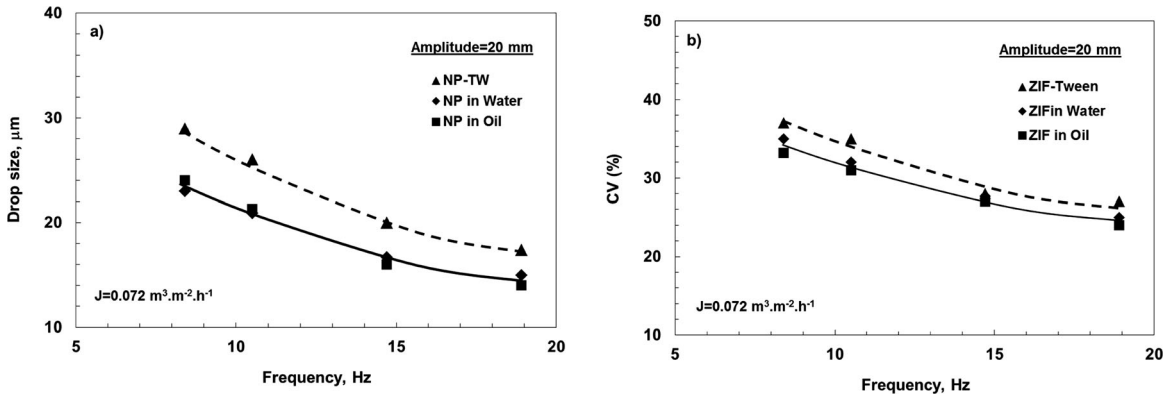

Fig. 10 Emulsions stabilized with ZIF-8 in the presence of the Tween-20 surfactant. Effect of oscillation frequency on (a) droplet size and (b) size distribution (CV).

As can be seen, the presence of surfactants did not significantly affect the average droplet size, but improved the distribution. This could possibly be attributed to a possible surfactant–NP synergy in stabilizing the droplets and reducing their coalescence and/or breakage probability. The results for emulsions stabilized with Tween-20 and ZIF-8 NPs are shown in Fig. 10a and b. In contrast to MIL-101, both larger droplet size and higher CV values are seen for ZIF-8. This may be explained by the possible NP interactions with the surfactant hydrophobic terminus which may have resulted in decreasing the affinity of both to the surface and consequently affecting the droplet size and stability. This further supports the assumption of surfactant interaction with both the liquid–liquid and the solid–liquid interfaces.

As discussed before, the effect of surfactant–NP interaction on emulsion properties, which has been observed by previous investigators, may be explained based on the fact that apart from a possible surfactant adsorption onto the NP which would limit its effectiveness, a surfactant may also displace NPs from the interface. This was confirmed by Vashisth, *et al.*,[46] who reported that application of shear resulted in displacing silica nanoparticles from the interface and the response of the latter to shear and deformation changed with surfactant concentration as it continues to displace the nanoparticles. It was also reported that the displacement process is not instant, but spans over a time period during which larger droplets are formed that would then breakup to sizes comparable to those of droplets stabilized by the surfactant alone. In another investigation by Binks *et al.*,[47] it was found that stirring solutions of nonionic surfactants with particle-stabilised emulsions increased droplet coalescence as the surfactant adsorbed onto the particle surfaces and caused aggregation. Both of the mentioned investigations support the hypothesis of a possible change in emulsion size distribution due to surfactant interaction with NPs at the droplet surface, which could lead to possible coalescence of the latter to a larger size followed by fragmentation under the effect of shear and/or flow eddies.

Comparison between measured and predicted droplet size

As mentioned earlier, droplet detachment in membrane emulsification occurs when the shear force F_d created by the relative motion between the fluid and the surface exceeds the interfacial tension holding force F_s. The latter is given by,

$$F_s = \pi d_p \gamma \tag{4}$$

For small droplets, the shear force acting on the droplet F_d may be approximated by,

$$F_d = (3/2) k_s \pi \tau d^2 \tag{5}$$

In the above equations, d_p is the pore diameter, and d is the droplet diameter. The factor k_s is a wall correction factor, which for a sphere moving parallel to the solid wall in a simple shear flow is ~ 1.7.[48] For a surface oscillating harmonically with velocity $u_o = a\omega \cos \omega t$, in which a is the oscillation amplitude and ω is the angular frequency, the velocity u of the fluid layer adjacent to the surface is given by the Stokes solution,[49]

$$u = u_o e^{-\eta} \cos(\omega t - \eta) \tag{6}$$

From which, the maximum shear stress τ is,

$$\tau = a\omega^{3/2} (\rho_c \nu_c^{1/2}) \tag{7}$$

where $\eta = y/\delta_s\, y$, the distance from the surface, $\delta_s = \sqrt{2\nu_c/\omega}$, and ν_c and ρ_c are the continuous phase kinematic viscosity, and density, respectively. If the shape of the droplet can still be approximated by a sphere before detachment, and neglecting other forces such as static, lift, and buoyancy forces, the droplet diameter may be estimated from a torque balance (TB) between the drag and interfacial tension forces using,[50]

$$F_d \sqrt{\left(\frac{d}{2}\right)^2 - \left(\frac{d_p}{2}\right)^2} = F_s \left(\frac{d_p}{2}\right) \tag{8}$$

Substituting the drag and interfacial tension forces and solving gives,

$$d = \frac{\left[\tau^2 d_p^{\,2} \left(\gamma + \sqrt{\gamma^2 - 3\tau^2 d_p^{\,2}}\right)\right]^{1/3}}{3^{2/3}\tau} + \frac{\tau d_p^{\,2}}{3^{1/3}\left[\tau^2 d_p^{\,2} \left(\gamma + \sqrt{\gamma^2 - 3\tau^2 d_p^{\,2}}\right)\right]^{1/3}} \tag{9}$$

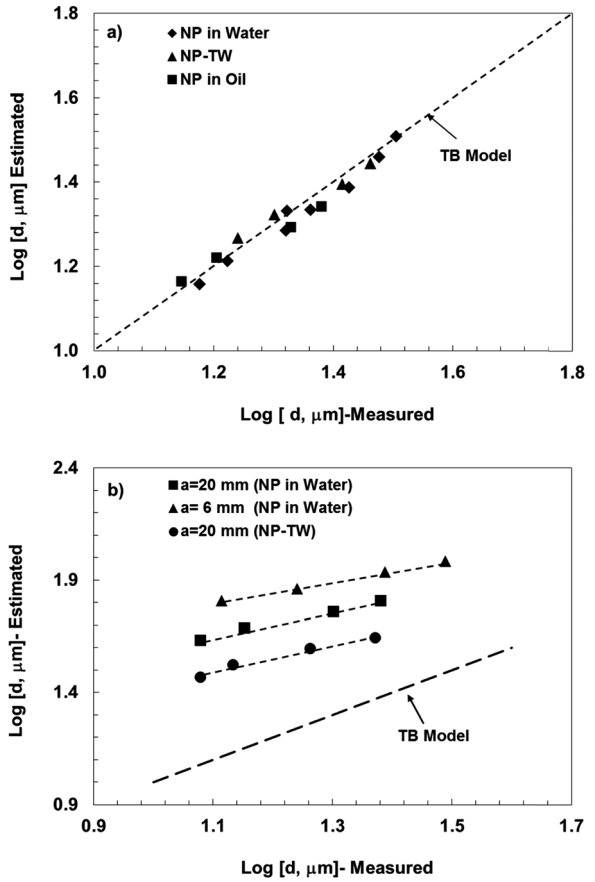

Fig. 11 Comparison between measured drop size and that predicted by the TB model for emulsion stabilized by (a) ZIF-8 NPs and (b) MIL-101 NPs.

To simplify by assuming the drag force to act at the droplet centre, a torque balance becomes,

$$F_{\mathrm{d}}\left(\frac{d}{2}\right) = F_{\mathrm{s}}\left(\frac{d_{\mathrm{p}}}{2}\right) \tag{10}$$

Substituting the drag and interfacial tension forces gives,

$$\left(\frac{3}{2}\right)k_{\mathrm{s}}\pi\tau d^2\left(\frac{d}{2}\right) = \pi d_{\mathrm{p}}\gamma\left(\frac{d_{\mathrm{p}}}{2}\right) \tag{11}$$

Defining the dimensionless droplet size $\xi = d/d_{\mathrm{p}}$, eqn (11) reads,

$$\left(\frac{3}{2}\right)k_{\mathrm{s}}\xi^3 {d_{\mathrm{p}}}^3\tau = {d_{\mathrm{p}}}^2\gamma \tag{12}$$

Rearranging gives,

$$\xi = \sqrt[3]{\frac{2\gamma}{3k_{\mathrm{s}}\tau d_{\mathrm{p}}}} \tag{13}$$

Fig. 11a and b show the comparison between measured droplet size and those predicted by the TB model for emulsions stabilized by ZIF-8 and MIL-101 NPs, respectively.

As can be seen, the former gives a good fit to the model predictions, while the latter deviates significantly. As discussed above, the simple TB model considers only the forces acting on a droplet during its formation until detachment, assuming that the system interfacial properties remain unchanged throughout this time span. Accordingly, the model will fail to predict the average droplet size if the system interfacial characteristics change during such a period due to for example, desorption of the stabilizing particles. Under these conditions, other mechanisms such as droplet breakage and/or coalescence may be triggered by the system hydrodynamics, which would result in changing the final emulsion average droplet size. We believe this to be the likely cause for the deviation of the TB model predictions for emulsions stabilized by MIL-101 NPs, which are less hydrophobic than ZIF-8 with lower affinity to the interface, and would be easier to detach from a droplet surface under the influence of the surrounding hydrodynamic forces leading to formation of larger droplets. Such droplets will have higher tendency for breakage into smaller satellite ones, particularly at higher oscillation intensities, and even possible coalescence of the formed satellite droplets into larger ones. This would result in significant changes to the originally formed emulsion droplets that cannot be predicted by simple TB analysis and is currently being investigated by our group.

Conclusions

This investigation demonstrates the possibility of successfully preparing Pickering emulsions stabilized by MIL-101 and ZIF-8 metal organic framework nanoparticles both in the presence and the absence of surfactants using a novel design oscillatory woven metal microscreen (WMMS) emulsification system. The results showed that both the system hydrodynamics and the hydrophobic/hydrophilic nature of the NPs influenced the interfacial properties of the oil–water interface during droplet formation and after detachment which affected the final droplet size and distribution. The strong hydrophobic nature of ZIF-8 NPs resulted in higher affinity to the surface, and formation of smaller and more stable droplets that resisted further breakage at high oscillation intensities. MIL-101 NPs on the other hand and due to their weaker hydrophobic nature resulted in the formation of larger and less stable droplets with more tendency for breakage into smaller satellite droplets, particularly at intense oscillations. Such a difference was also noticed when using surfactants, where synergy was observed with MIL-101 in both droplet size and stability through interfacial tension reduction and possible larger surface coverage. Compared to ZIF-8, larger droplets and wider distribution were observed, likely due to surfactant interaction with the NP, which resulted in decreasing surface coverage, and increasing interfacial tensions.

Nomenclature

a	Oscillation amplitude (m).
A	Interfacial area (m^2)
CV	Coefficient of variation (%)
d	Average droplet size (m).
d_{p}	Pore diameter (m).

E_d	Desorption energy required to remove one NP from the interface (J)
ΔE	Change in interfacial energy (J)
f	Oscillation frequency (Hz)
F_d	Shear force (N)
F_s	Interfacial tension holding force (N)
J	Dispersed phase flux ($m^3\ m^{-2}\ h^{-1}$)
k_s	Wall correction factor (—).
N	Number of droplets (—).
N_p	Number of NPs in a given interfacial area A (—)
R	NP radius (m).
t	Time (s)
u	Continuous phase velocity at the droplet centre ($m\ s^{-1}$).
y	Distance from the surface (m)
γ	Interfacial tension ($N\ m^{-1}$).
η	Dimensionless distance from the surface (—)
δ_s	Stokes layer thickness (m)
θ	Particle contact angle with the oil–water interface (Rad)
ν_c	Continuous phase kinematic viscosity ($m^2\ s^{-1}$).
ρ_c	Continuous phase density ($kg\ m^{-3}$)
τ	Shear stress (Pa)
ξ	Dimensionless droplet size (—)
ω	Angular frequency (s^{-1})

Acknowledgements

The authors are grateful to the Natural Sciences and Engineering Research Council of Canada for the financial support. Grant # 238635-2012.

References

1 T. Welss, D. A. Basketter and K. R. Schröder, *Toxicol. In Vitro*, 2004, **18**, 231–243.
2 R. Aveyard, B. P. Binks and J. H. Clint, *Adv. Colloid Interface Sci.*, 2003, **100–102**, 503–546.
3 S. Jiang, Q. Chen, M. Tripathy, E. Luijten, K. S. Schweizer and S. Granick, *Adv. Mater.*, 2010, **22**, 1060–1071.
4 Y. Chevalier and M.-A. Bolzinger, *Colloids Surf., A*, 2013, **439**, 23–34.
5 Y. He, *Mater. Lett.*, 2005, **59**, 114–117.
6 J. Li and H. D. H. Stöver, *Langmuir*, 2010, **26**, 15554–15560.
7 B. P. Binks and S. O. Lumsdon, *Langmuir*, 2000, **16**, 2539–2547.
8 T. A. L. Do, J. R. Mitchell, B. Wolf and J. Vieira, *React. Funct. Polym.*, 2010, **70**, 856–862.
9 S. U. Pickering, *J. Chem. Soc. Trans.*, 1907, **91**, 2001–2021.
10 B. P. Binks and S. O. Lumsdon, *Langmuir*, 2001, **17**, 4540–4547.
11 J. R. Long and O. M. Yaghi, *Chem. Soc. Rev.*, 2009, **38**, 1213–1214.
12 Q. Yuan, O. J. Cayre, M. Manga, R. A. Williams and S. Biggs, *Soft Matter*, 2010, **6**, 1580–1588.
13 G. T. Vladisavljević and R. A. Williams, *Adv. Colloid Interface Sci.*, 2005, **113**, 1–20.
14 A. J. Gijsbertsen-Abrahamse, A. van der Padt and R. M. Boom, *J. Membr. Sci.*, 2004, **230**, 149–159.
15 E. Haque, N. A. Khan, J. H. Park and S. H. Jhung, *Chem. – Eur. J.*, 2010, **16**, 1046–1052.
16 J. Lee, O. K. Farha, J. Roberts, K. A. Scheidt, S. T. Nguyen and J. T. Hupp, *Chem. Soc. Rev.*, 2009, **38**, 1450–1459.
17 S. Bourrelly, P. L. Llewellyn, C. Serre, F. Millange, T. Loiseau and G. Férey, *J. Am. Chem. Soc.*, 2005, **127**, 13519–13521.
18 H. G. Gomaa, J. Liu, R. Sabouni and J. Zhu, *Chem. Eng. Sci.*, 2014, **117**, 161–172.
19 H. G. Gomaa, J. Liu, R. Sabouni and J. Zhu, *Colloids Surf., A*, 2014, **456**, 160–168.
20 W. Zeng, H. G. Gomaa, J. Liu and J. Zhu, *Chem. Eng. Process.*, 2013, **73**, 111–118.
21 G. T. Vladisavljević and R. A. Williams, *J. Colloid Interface Sci.*, 2006, **299**, 396–402.
22 V. Schadler and E. J. Windhab, *Desalination*, 2006, **189**, 130–135.
23 M. S. Manga, O. J. Cayre, R. A. Williams, S. Biggs and D. W. York, *Soft Matter*, 2012, **8**, 1532–1538.
24 N. Aryanti, R. Hou and R. A. Williams, *J. Membr. Sci.*, 2009, **326**, 9–18.
25 J. Zhu and D. Barrow, *J. Membr. Sci.*, 2005, **261**, 136–144.
26 R. G. Holdich, M. M. Dragosavac, G. T. Vladisavljević and S. R. Kosvintsev, *Ind. Eng. Chem. Res.*, 2010, **49**, 3810–3817.
27 E. Egidi, G. Gasparini, R. G. Holdich, G. T. Vladisavljević and S. R. Kosvintsev, *J. Membr. Sci.*, 2008, **323**, 414–420.
28 K. L. Thompson, S. P. Armes and D. W. York, *Langmuir*, 2011, **27**, 2357–2363.
29 K. S. Park, Z. Ni, A. P. Côté, J. Y. Choi, R. Huang, F. J. Uribe-Romo, H. K. Chae, M. O'Keeffe and O. M. Yaghi, *Proc. Natl. Acad. Sci. U. S. A.*, 2006, **103**, 10186–10191.
30 K. M. L. Taylor-Pashow, J. D. Rocca, Z. Xie, S. Tran and W. Lin, *J. Am. Chem. Soc.*, 2009, **131**, 14261–14263.
31 R. Ananthoji, J. F. Eubank, F. Nouar, H. Mouttaki, M. Eddaoudi and J. P. Harmon, *J. Mater. Chem.*, 2011, **21**, 9587–9594.
32 I. B. Vasconcelos, T. G. d. Silva, G. C. G. Militao, T. A. Soares, N. M. Rodrigues, M. O. Rodrigues, N. B. d. Costa, R. O. Freire and S. A. Junior, *RSC Adv.*, 2012, **2**, 9437–9442.
33 C. Y. Sun, C. Qin, X.-L. Wang, G.-S. Yang, K.-Z. Shao, Y.-Q. Lan, Z.-M. Su, P. Huang, C.-G. Wang and E.-B. Wang, *Dalton Trans.*, 2012, **41**, 6906–6909.
34 K. M. L. Taylor-Pashow, J. D. Rocca, Z. Xie, S. Tran and W. Lin, *J. Am. Chem. Soc.*, 2009, **131**, 14261–14263.
35 P. Horcajada, T. Chalati, C. Serre, B. Gillet, C. Sebrie, T. Baati, J. F. Eubank, D. Heurtaux, P. Clayette, C. Kreuz, J.-S. Chang, Y. K. Hwang, V. Marsaud, P.-N. Bories, L. Cynober, S. Gil, G. Ferey, P. Couvreur and R. Gref, *Nat. Mater.*, 2010, **9**, 172–178.
36 M. Hartmann and M. Fischer, *Microporous Mesoporous Mater.*, 2012, **164**, 38–43.
37 G. Férey, C. Mellot-Draznieks, C. Serre, F. Millange, J. Dutour, S. Surblé and I. Margiolaki, *Science*, 2005, **309**, 2040–2042.

38 S. Cao, T. D. Bennett, D. A. Keen, A. L. Goodwin and A. K. Cheetham, *Chem. Commun.*, 2012, **48**, 7805–7807.
39 H. Fan and A. Striolo, *Phys. Rev. E: Stat., Nonlinear, Soft Matter Phys.*, 2012, **86**, 051610.
40 C. P. Whitby, D. Fornasiero and J. Ralston, *J. Colloid Interface Sci.*, 2008, **323**, 410–419.
41 H. Nciri, N. Huang, V. Rosilio, M. Trabelsi-Ayadi, M. Benna-Zayani and J.-L. Grossiord, *Rheol. Acta*, 2010, **49**, 961–969.
42 F. Ravera, M. Ferrari, L. Liggieri, G. Loglio, E. Santini and A. Zanobini, *Colloids Surf., A*, 2008, **323**, 99–108.
43 Q. Lan, F. Yang, S. Zhang, S. Liu, J. Xu and D. Sun, *Colloids Surf., A*, 2007, **302**, 126–135.
44 H. Ma, M. Luo and L. L. Dai, *Phys. Chem. Chem. Phys.*, 2008, **10**, 2207–2213.
45 F. Ravera, E. Santini, G. Loglio, M. Ferrari and L. Liggieri, *J. Phys. Chem. B*, 2006, **110**, 19543–19551.
46 C. Vashisth, C. P. Whitby, D. Fornasiero and J. Ralston, *J. Colloid Interface Sci.*, 2010, **349**, 537–543.
47 B. P. Binks, A. Desforges and D. G. Duff, Synergistic stabilization of emulsions by a mixture of surface-active nanoparticles and surfactant, *Langmuir*, 2007, **23**, 1098–1106.
48 A. J. Goldman, R. G. Cox and H. Brenner, *Chem. Eng. Sci.*, 1967, **22**, 653–660.
49 H. Schlichiting, *Boundary-Layer Theory*, McGraw-Hill Book, Company, New York, 7th edn, 1979, p. 93.
50 S. R. Kosvintsev, G. Gasparini, R. G. Holdich, I. W. Cumming and M. T. Stillwell, Liquid-Liquid Membrane Dispersion in a Stirred Cell with and without Controlled Shear, *Ind. Eng. Chem. Res.*, 2005, **44**, 9323–9330.

